Molecular dynamics with quantum forces: Vibrational spectra of localized systems

James R. Chelikowsky and Xiaodun Jing
Department of Chemical Engineering and Materials Science, Minnesota Supercomputer Institute, University of Minnesota, Minneapolis, Minnesota 55455

K. Wu and Y. Saad
Department of Computer Science, Minnesota Supercomputer Institute, University of Minnesota, Minneapolis, Minnesota 55455

(Received 9 November 1995)

We present molecular-dynamics simulations with quantum forces for localized systems using a real-space method. We illustrate calculations for the vibrational modes of small molecules and clusters. Unlike other real-space methods using adaptive grids, this procedure does not require any Pulay corrections for the forces, nor does it suffer from the complication of redefining a grid after each time step of the molecular-dynamics simulation. Our method is based on combining higher order finite difference methods with *ab initio* pseudopotentials. We also introduce an iterative diagonalization scheme based on preconditioned Krylov techniques. Compared to *plane-wave–supercell methods*, this method is more efficient and simpler to implement. Examples are presented for the CO_2 molecule and a silicon cluster, Si_4.

I. INTRODUCTION

One of the outstanding achievements in computational physics in the past decade has been the development of *ab initio* methods for determining the structural properties of condensed-matter systems.[1] This development has led to a number of innovative approaches, e.g., the development of ''quantum'' molecular dynamics and the application of *first-principles* methods to realistic systems such as liquids, clusters, amorphous solids, and glasses.[2] For the most part, this work has been based on traditional solid-state methods which combine pseudopotentials, plane waves, and supercell geometries for localized systems.[3] While these approaches have achieved much success, the drawbacks of the *plane-wave–supercell* approach are notable. A plane-wave basis is required to replicate not only the electronic states of the localized system of interest, but also ''vacuum'' regions imposed by the supercell geometry. The vacuum region must be large to avoid ''cell-cell'' interactions, but replicating the vacuum in the supercell for a localized system can be almost as costly as replicating the system itself. An additional complication that arises with the use of plane waves concerns the use of fast Fourier transforms (FFT) for handling the convolutions. While FFT's are a great advantage in expediting the calculation, these transforms present computational communication obstacles when one attempts to implement them on parallel computer architectures.

A number of approaches have been proposed to circumvent or mitigate the deficiencies of the plane-wave–supercell method. For example, Euclidean grids, adaptive grids, multigrids, wavelets, and other ''real-space'' methods have recently been proposed.[4] These methods are still in an embryonic state when compared to the traditional approach of plane waves, but they promise a new direction and have been quite successful for a number of prototypical systems.

Here we illustrate a real-space method for performing ''quantum'' molecular-dynamics on localized systems. In particular, we concentrate on demonstrating the efficiency of this method for some localized systems such as the CO_2 molecule and a cluster of silicon. With respect to the CO_2 molecule, it has been questioned whether simple Euclidean real-space grids can be efficient for such systems.[5] We will demonstrate that regular grids possess some significant advantages over adaptive grids and that CO_2 can be handled in a simple and direct fashion. We also consider a small silicon cluster for which the vibrational modes have been calculated by real-space methods via a determination of the dynamical matrix.[6] This will allow us to compare ''static'' and ''dynamical'' calculations for the vibrational modes.

There are several advantages in using Euclidean grids. For example, no complications arise in determining the interatomic forces as would be the case for adaptive grids, e.g., Pulay forces.[7] Moreover, the grids do not have to be updated as the simulation proceeds. This can be a cumbersome process as, in principle, the grids should be reconfigured for each molecular-dynamics simulation time step.[8] It might be argued that adaptive grids are a better representation for localized systems as the ''basis'' can be adjusted to regions where the wave functions are highly localized and where they are not. However, this adjustment is nontrivial. Often, fictitious elastic terms are used to accelerate the optimization of the mesh near the nuclei, or ion core.[9] While adaptive grid methods may be appropriate for some systems, e.g., first row elements, or transition metals, we would argue an adaptive mesh complicates the procedure enormously.

Another advantage of Euclidean grids concerns the nature of the resulting eigenvalue problem. The resulting matrix is sparse and regularly structured. Owing to these attributes, simple operations with the matrix, such as matrix-by-vector products can be done efficiently on vector processors as well

as in multiprocessing environments. In fact, the contribution to the matrix which is due to the Laplacian does not even need to be stored. Whenever a matrix-vector-product is invoked, the corresponding finite difference operation can be performed directly on the mesh points. The coefficients of the finite difference approximation are the same for each point. The nonlocal components of the pseudopotential do not cause major difficulties. The related contributions to the product of a matrix by a vector consists of an irregular computation which is similar to the product of a small sparse matrix by a vector.

II. INTERATOMIC FORCES

Within the local density approximation, the total ground-state energy is given by

$$E_{\rm tot}=T[\rho]+E_{e-i}(\mathbf{R}_a,[\rho])+E_{\rm hart}[\rho]+E_{\rm xc}[\rho]+E_{i-i}(\mathbf{R}_a), \tag{1}$$

where the atomic positions are given by $\mathbf{R}_a$ and $\rho(\mathbf{r})$ is the charge density. $T[\rho]$ is the kinetic energy, $E_{e-i}(\mathbf{R}_a,[\rho])$ is the electron-ion potential energy, $E_{\rm hart}[\rho]$ is the Hartree or Coulomb potential energy, $E_{\rm xc}[\rho]$ is the exchange-correlation energy, and $E_{i-i}(\mathbf{R}_a)$ is the ion-ion potential energy. We have implicity assumed the Born-Oppenheimer approximation in writing Eq. (1). $E_{\rm tot}$ is a functional of the electron density, $\rho(\mathbf{r})$, for the electronic ground state.

The force on an atom is the first-order derivative of total energy with respect to its coordinate, and is given by applying the Hellmann-Feynman[10] theorem. The total force, F_a^α, on an atom located at $\mathbf{R}_a$ in the α direction is given by

$$F_a^\alpha=-\frac{\partial E_{e-i}}{\partial R_a^\alpha}-\frac{\partial E_{i-i}}{\partial R_a^\alpha}. \tag{2}$$

$E_{i-i}(\mathbf{R}_a)$, the interionic core energy, is simply the point-charge–point-charge interaction under the ''frozen core'' approximation.

If we consider a pseudopotential representation of the ion-core, $V_{\rm ion}$, the potential term corresponds to a nonlocal operator, i.e., the potential depends on the angular momentum of the wave function upon which it operates. In general, the pseudopotential can be decomposed into a part which is local and a part which is nonlocal. In real space, this formalism may be cast into the following form:[11–13]

$$\begin{aligned}V_{\rm ion}(\mathbf{r})=&\sum_a V_{\rm ion,loc}(|\mathbf{r}_a|)\\&+\sum_{a,n,lm}\frac{1}{\langle\Delta V_{lm}^a\rangle}|\Delta V_{{\rm ion},l}(r_a)u_{lm}(\mathbf{r}_a)\rangle\\&\times\langle\Delta V_{{\rm ion},l}(r_a')u_{lm}(\mathbf{r}_a')|,\end{aligned} \tag{3}$$

where $\langle\Delta V_{lm}^a\rangle$ is a normalization factor,

$$\langle\Delta V_{lm}^a\rangle=\int u_{lm}(\mathbf{r}_a)\Delta V_{{\rm ion},l}(r_a)u_{lm}(\mathbf{r}_a)d^3r, \tag{4}$$

and $\mathbf{r}_a=\mathbf{r}-\mathbf{R}_a$, u_{lm} are the atomic pseudopotential wave functions of angular and azimuthal momentum quantum numbers (l,m) from which the l-dependent ionic pseudopotentials $V_{{\rm ion},l}(r)$ are generated. We have made the assumption that the ion core is spherically symmetric (which is a good approximation for the systems of interest here). $\Delta V_{{\rm ion},l}(r)=V_{{\rm ion},l}(r)-V_{\rm ion,loc}(r)$ is the difference between the l component of the ionic pseudopotential and the local ionic potential. The energy from the electron-ion interaction, E_{e-i} can be obtained by using Eq. (3) as

$$\begin{aligned}E_{e-i}=&\sum_n^{\rm occ}\int\psi_n(\mathbf{r})V_{\rm ion}(\mathbf{r})\psi_n(\mathbf{r})d^3r\\=&\sum_a\int\rho(\mathbf{r})V_{\rm ion,loc}(r_a)d^3r\\&+\sum_{a,n,lm}\frac{1}{\langle\Delta V_{lm}^a\rangle}[G_{nlm}^a]^2,\end{aligned} \tag{5}$$

where

$$G_{n,lm}^a=\int\Delta V_l(r_a)u_{lm}(\mathbf{r}_a)\psi_n(\mathbf{r})d^3r. \tag{6}$$

The $\psi_n(\mathbf{r})$ are the eigenwave functions of a one-electron Schrödinger equation, and the sum on n is over the occupied states. Combining Eqs. (2) and (5), one can get an expression for the force,

$$\begin{aligned}F_a^\alpha=&\int\rho(\vec{r})\frac{\partial V_{\rm ion,loc}(r_a)}{\partial r_a^\alpha}d^3r+2\sum_{n,lm}\frac{1}{\langle\Delta V_{lm}^a\rangle}G_{n,lm}^a\frac{\partial G_{n,lm}^a}{\partial r_a^\alpha}\\&-\frac{\partial E_{i-i}}{\partial R_a^\alpha}.\end{aligned} \tag{7}$$

The force from the electronic contribution comprises two parts. The first term at the right-hand side of Eq. (7) is the contribution from the local ionic potential, and the second term is from the nonlocal potential. It is possible to accelarate convergence of these forces by using the procedure of Chan, Bohnen, and Ho.[14]

Once the eigenvalues and vectors of the system are determined, the interatomic quantum forces can be trivially evaluated. The forces can then be utilized in performing molecular dynamics with quantum forces.

III. REAL-SPACE METHODS FOR SOLVING THE SCHRÖDINGER EQUATION

In previous work, we have outlined a real-space method for solving a one-electron Schrödinger equation. Here we overview the main features of the method and introduce some modifications to it which greatly enhance the computational efficiency of the procedure.

Unlike the traditional approach in which the wave functions are expressed with a basis, e.g., plane waves, we employ a finite difference approach. A key aspect of our work is the availability of *higher-order finite difference expansions* for the kinetic energy operator, i.e., expansions of the Laplacian. A uniform grid is imposed on our system, using mesh points that are described in a finite domain by (x_i,y_j,z_k). We approximate $\partial^2\psi/\partial x^2$ at (x_i,y_j,z_k) by

$$\frac{\partial^2\psi}{\partial x^2}=\sum_{n=-N}^{N} C_n\psi(x_i+nh,y_j,z_k)+O(h^{2N+2}), \qquad (8)$$

where h is the grid spacing and N is a positive integer. This approximation is accurate to $O(h^{2N+2})$ upon the assumption that ψ can be approximated by a power series in h. Algorithms are available to compute the coefficients C_n for arbitrary order in h.[16]

With the kinetic energy operator expanded as in Eq. (8), one can set up a one-electron Schrödinger equation over the grid. We have assumed a uniform grid over the three dimensions. This is not a necessary assumption, but in most cases it is the most efficient and convenient. We approximate $\psi(x_i,y_j,z_k)$ on the grid by solving the secular equation:

$$-\frac{\hbar^2}{2m}\left[\sum_{n_1=-N}^{N} C_{n_1}\psi_n(x_i+n_1h,y_j,z_k)+\sum_{n_2=-N}^{N} C_{n_2}\psi_n(x_i,y_j+n_2h,z_k)+\sum_{n_3=-N}^{N} C_{n_3}\psi_n(x_i,y_j,z_k+n_3h)\right]$$
$$+[V_{\rm ion}(x_i,y_j,z_k)+V_H(x_i,y_j,z_k)+V_{\rm xc}(x_i,y_j,z_k)]\psi_n(x_i,y_j,z_k)=E_n\psi_n(x_i,y_j,z_k). \qquad (9)$$

$V_{\rm ion}$ is the nonlocal ionic pseudopotential as in the previous section, V_H is the Hartree potential, and $V_{\rm xc}$ is the local-density expression for the exchange and correlation potential. Two parameters used in setting up the matrix are the grid spacing h, and the order N.

Several issues must be addressed when solving Eq. (9). The first concerns the procedure by which the self-consistent field is constructed. The exchange-correlation potential, $V_{\rm xc}$, is constructed trivially once the charge density has been obtained over the grid. However, the Hartree potential is nontrivial and requires the solution of the Poisson equation:

$$\nabla^2 V_H(\mathbf{r})=4\pi\rho(\mathbf{r}). \qquad (10)$$

The Hartree potential can be determined in several ways, e.g., by a direct summation over the grid, or by setting up a matrix equation and solving with direct or iterative methods. For small systems, the simplest and easiest approach is to perform the direct summation over all the grid points. However, once the grid size exceeds $\sim 10^4$ grid points, it is more efficient and *accurate* to use either FFT transforms or iterative methods. In our work, we use a preconditioned conjugate gradient method to solve Eq. (10). The boundary conditions required for a solution of Eq. (10) are determined by a multipole expansion of the pseudocharge density outside of a given spherical region. Typically, monopole, dipole, and quadrupole terms are sufficient to yield an accurate solution. The savings obtained by this procedure can be dramatic when compared to a direct summation. For example, in the case of the CO_2 molecule, approximately 96 000 grid points were used. A direction summation solution for V_H required roughly two orders of magnitude more computational time than did the conjugate gradient solution. We use an Anderson mixing scheme to expedite the convergence of the self-consistent field.[17]

Another issue concerns the nonlocality of the ionic pseudopotential. Usually, one component is taken as the local component. Here we take $V_{\rm loc}=V_s$, where V_s is the s component. We may ignore contributions to the potential higher than $l=1$ for the elements of interest here (i.e., carbon, oxygen, and silicon). This choice has been verified by direct comparisons with calculations using a plane-wave basis. The integral $G^a_{n,lm}$ [Eq. (6)] involving $\psi_n(x,y,z)$ is performed over the grid. We have

$$\int u_{lm}(x,y,z)\Delta V_l(x,y,z)\psi_n(x,y,z)dx\ dy\ dz$$
$$=\sum_{ijk} u_{lm}(x_i,y_j,z_k)\Delta V_l(x_i,y_j,z_k)\psi_n(x_i,y_j,z_k)h^3. \qquad (11)$$

Equation (9) is a matrix eigenvalue problem. The size M of the matrix A resulting from this eigenvalue problem is equal to the number of grid points. For these isolated systems the matrix is real, symmetric, and sparse. The degree of sparsity of the matrix depends on the order N to which the kinetic energy is expanded. From Eq. (9), the kinetic energy term contributes at most $3(2N+1)$ nonzero elements for each row. We must add to these a number of terms coming from the nonlocal pseudopotential. These nonlocal contributions depend on the number and nature of the atomic species present, and the location in space. The other potentials do not contribute new nonzero elements but modify the main diagonal of the matrix.

Several efficient techniques developed in the literature can be used to solve sparse eigenvalue problems such as the one above; see for example Ref. 18. Two popular such procedures are the accelerated subspace iteration and the Lanczos algorithm. Both methods consist of projecting the original problem into a small subspace in which standard techniques can be used. For example, in the simplest version of the subspace iteration algorithm, an initial basis $X_0=[x_0,x_1,\ldots,x_m]$ is chosen and the matrix $X_k=A^kX_0$ is formed for a certain power k. Then, a Ritz procedure is applied to A with this matrix. This means that X_k is orthonormalized into a matrix Y_k and the eigenvalues λ_i and eigenvectors ϕ_i of the small $m\times m$ projected matrix $Y_k^TAY_k$ are computed by a standard method such as the QR algorithm.[18] The eigenvalues λ_i are then used as approximations to the eigenvalues of A and the vectors $Y_k\phi_i$ are used as approximations to the eigenvectors of A. The procedure is repeated with X replaced by the set of approximate eigenvectors until convergence is reached. In realistic implementations of this procedure, it is common to use a Chebyshev polynomial

$C_k(A)$ instead of the powers A^k to obtain the next basis X_k from X. The Lanczos algorithm also utilizes a Ritz procedure. However, the basis used consists of the successive powers $A^k v_0, k=1,\ldots,m$ where v_0 is an initial vector. In this case, the dimension m increases at each step.

Both the Lanczos and subspace iteration procedures can and should be ''preconditioned'' to improve convergence rates.[19] Preconditioning consists of enhancing a given vector introduced in the new basis by a process which amplifies the desired eigenvector components and dampens the others. The most common way to achieve this is to perform a shift-and-invert procedure. In this strategy, the problem solved is

$$(A-\sigma I)^{-1}u=\theta u.$$

The eigenvectors of the shifted and inverted matrix are the same as those of A. Its eigenvalues which are transformed from those of A via a simple rational transformation have typically a much better separation around the value σ. This results in much better convergence rates. In typical shift-and-invert procedures the matrix $(A-\sigma I)$ is factored (using LDL^T factorization) every time the shift σ is changed. This factorization step may be prohibitively expensive for large matrices. As a result, the preferred alternative is to use a preconditioned Lanczos-type procedure to construct a subspace based on $M^{-1}A$ where M is some preconditioner. The resulting basis is then used for a Ritz projection, similarly to what was described above. The preconditioner M is an approximation to $(A-\sigma I)$. In fact the preconditioner M can vary at each step, i.e., for each basis vector to be determined. This permits the use of preconditioners that depend on specific eigenvalues, as better approximations of these eigenvalues are extracted from the algorithm. In the Davidson algorithm the matrix M is taken to be simply $D-\sigma_i$ in which D is the diagonal of A, and σ_i is the most current approximation of the eigenvalue which is being targeted.

From a practical viewpoint, an important observation is that the diagonalization algorithms use the coefficient matrix A only to perform matrix-by-vector products. The sparse matrix A can be stored in one of several sparse formats available[19] which avoid storing the zero elements. Performing matrix-vector products with these formats is inexpensive. However, because of the special structure of the matrix, a better alternative is to perform these matrix vector products in ''stencil'' or ''operator'' form.[20] Indeed, as is clear from Eq. (9) the matrix-by-vector kinetic operations can easily be performed by accessing the desired components of the current vector ψ and forming a small linear combination using the coefficients C_{n_i}. Only the constant coefficients $C_{n_i}, i=1,2,3; n=-N,N$ need to be known. Similarly, the nonlocal operations are accomplished by performing vector-by-vector operations. This strategy saves storage and leads to an efficient implementation on most high-performance vector and parallel computers.

IV. MOLECULAR-DYNAMICS SIMULATIONS USING QUANTUM FORCES

Our goal in this section is to illustrate the feasibility of using a real-space method to perform molecular-dynamics (MD) simulations to calculate vibrational modes in small molecules and clusters. Vibrational modes present strong challenges to any *ab initio* theory. The modes can be subtly interrelated and the energy of a cluster must be known to high precision for an accurate determination of the interatomic interactions.

A. Vibrational modes in CO_2

Traditionally, first row elements such as carbon or oxygen have been viewed as some of the most difficult elements for pseudopotential methods. Since no p states occur in the ion core for these elements, the resulting pseudopotential is highly nonlocal: the s and p states sense very different potentials. Moreover, their valence states are quite localized relative to those in the second row elements such as silicon or sulfur. For this reason, molecular systems such as CO_2 are often used as test cases for new numerical methods. Studies for this molecular system have recently been performed using plane-wave[5] and real-space[8] adaptive grids. The results of these studies were very promising in terms of treating this system. However, this work cast some doubt on the utility and efficacy of finite difference methods based on Euclidean grids. In particular, Gygi and Galli were not able to replicate the energy versus bond length of the CO_2 for a symmetric stretch with finite difference methods when compared to a real-space adaptive grid method.[8] They attributed this problem to inaccurate solution obtained when using a ''coarse'' Euclidean grid.

In setting up a grid for the CO_2 molecule, several grid spacings were examined. Previous work[11] with $h=0.4$ a.u. (1 a.u. = 0.529 Å) led to reasonable results for C_2, O_2, and CO; however, it was noted for CO that this grid spacing was probably insufficient for a fully converged solution.[11] Here we tested $h=0.3$ a.u. and $h=0.25$ a.u., the latter value was used in all our calculations as it appeared to produce a well converged result. Equating $(\pi/h)^2$ to a plane-wave cutoff would yield a corresponding plane-wave cutoff of 157 Ry. A plane-wave calculation for such a cutoff would be prohibitively expensive whereas in the finite difference approach, the problem is easily tractable. The CO_2 molecule was placed in a spherical domain of $R_{max}=7.1$ a.u. Wave functions outside of this region are constrained to vanish. This configuration results in 96 105 grid points. It is possible to use other boundary conditions. For example, for an axially symmetric molecule like CO_2, i.e., a linear molecule, a cylindrical boundary might be more appropriate and require fewer grid points.

In Fig. 1, we display the energy of the CO_2 versus bond length for a symmetric stretch. The equlibrium bond length was found to be 2.185 a.u. This is in excellent agreement with other procedures as indicated in Table I. Moreover, our calculation shows no evidence of a ''double hump'' as in the work of Gygi and Galli.[8] There are some technical differences between our work and theirs. Namely, the pseudopotential, grid spacing, and finite difference order were different in the two calculations. Our pseudopotential was determined by the Troullier-Martins method.[11,13] The work of Gygi and Galli used a Bachelet-Hamann-Schlüter potential.[21] We used $N=6$ to determine the finite difference order, they used $N=2$. They used a grid spacing of $h=0.21$ a.u., whereas we used $h=0.25$ a.u. From our experience, a

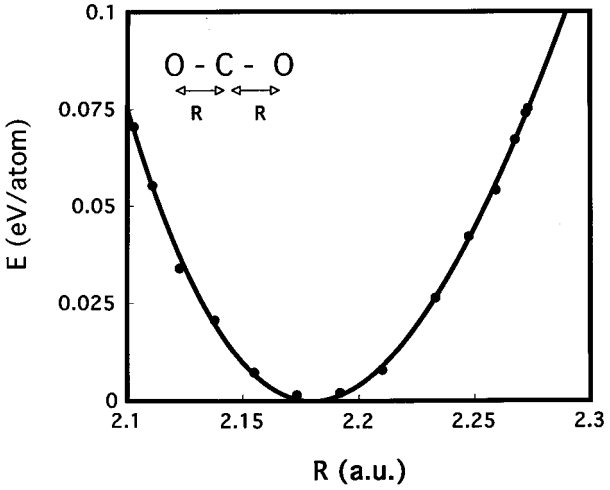

FIG. 1. Total energy of CO_2 molecule versus the C-O separation. The energy zero point is chosen at the equilibrium bond length. The energy versus volume points are fit to a cubic polynomial.

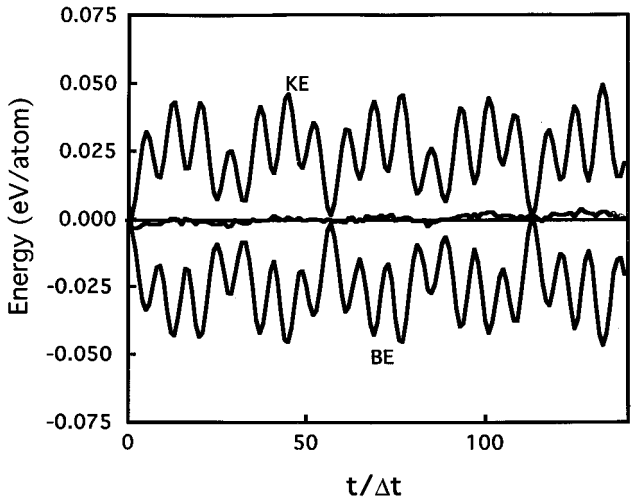

FIG. 2. MD simulation for the CO_2 molecule. The kinetic energy (KE) and binding energy (BE) are shown as a function of the simulation time. The total energy (KE+BE) is also shown with the zero taken as the time average of the total energy. The time step Δt is 0.85 fs.

coarse grid results in an energy versus bond length which has a larger curvature than a fine grid, but the general shape is otherwise unchanged. The Gygi and Galli result appears to be the result of the nature of the pseudopotential they employed[21] as opposed to an inherent deficiency of the Euclidean grid.[22]

To determine the vibrational modes of the molecule, we perform an MD simulation with quantum forces. To initiate the MD simulation, we proceed as in previous work.[5] We displaced the atomic positions of the CO_2 molecule away from the equilibrium geometry in an asymmetric manner. The largest displacement was ~ 0.1 a.u. The time step in our simulation was taken to be 0.85 fs or about 35 a.u. We allowed an equilibration time of 60 time steps followed by 140 time steps for the simulation during which the kinetic energy, binding energy, or Kohn-Sham energy, and trajectories of the particles were saved. In Fig. 2, the kinetic energy (KE), binding energy (BE), and the total energy are plotted over the simulation time. The total energy during the simulation shows some variation from ''discretization errors.'' This is to be expected since the introduction of a grid can break symmetry. However, we view this issue as tractable as the rms error in energy conservation is less than $\sim$ 1 meV/atom. More importanty, there is no significant drift over the simulation time. Any drift present is less than $\sim$ 1 meV/atom over the simulation run.

Using the time dependence of the kinetic energy, it is possible to calculate the vibrational spectra as in previous work which used a plane-wave–adaptive grid method.[5] We also use the method of maximum entropy to extract vibrational frequencies.[5] 150 poles were used in the fitting process. The resulting power spectrum of the vibrations of the CO_2 molecule are given in Fig. 3. The vibrational spectrum of the CO_2 molecule consists of two infrared-active modes (π_u, σ_u^+), and a Raman σ_g^+ doublet split by a Fermi resonance. The π_u corresponds to a bending mode and the σ_u^+ mode corresponds to an asymmetric stretch. The σ_g^+ corresponds to a symmetric stretch. As noted in previous work,[5] it is a challenge for any *ab initio* method to reproduce the splitting of the σ_g^+ mode. In Fig. 3, the σ_g^+ mode is much weaker than the other mode, perhaps because of our initial conditions, but the doublet in question is clearly present. The splitting of this mode has also been observed with adaptive grid methods[5,8] and represents a success of the local-density approximation. In Table I, we compare our calculated values with experiment and to the adaptive grid work.

We can also use our method to compute the atomization energy of the CO_2 molecule, i.e., the energy to dissociate the molecule into its constituent atoms. We find a value of atomization of $\sim$19.8 eV/m.u. as compared to a value of 16.7 eV/m.u. from experiment.[24] Our estimate is consistent with local-density theory in that the calculated atomization energy exceeds the experimental value by about $\sim$10–20%. This overestimate is also reassuring in that it suggests our grid

TABLE I. Equilibrium C-O bond length and vibrational frequencies in CO_2 calculated using a real-space finite difference pseudopotential method. These results are compared to adaptive grid methods and experiment. The bond length is in a.u. and the vibrational frequencies in cm^{-1}.

	C-O bond length	π_u	σ_g^+	σ_u^+
Adaptive grid plane waves (Ref. 5)		648	(1368,1428)	2353
Adaptive grid real space (Ref. 8)	2.198	648	1336	2374
Real-space Euclidean grid	2.185	663	(1379, 1456)	2355
Experiment (Ref. 23)	2.192	673	(1286,1388)	2349

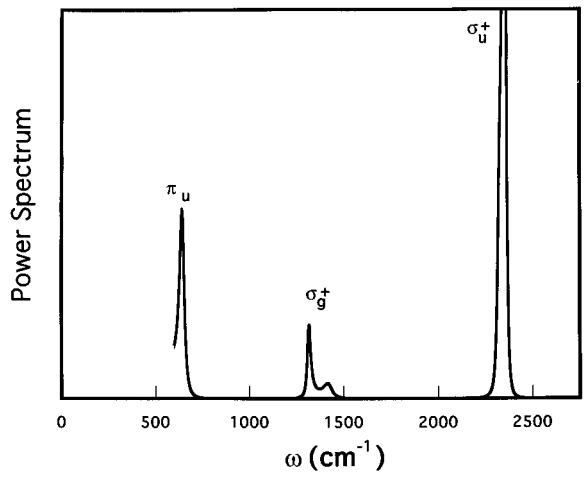

FIG. 3. Power spectrum of the vibrational modes for the CO_2 molecule.

results in a well converged solution. It is possible to improve this estimate for the heat of atomization by including gradient corrections, but this task is outside the scope of the paper. No value for this quantity was given in the adaptive grid work.[5,8]

Although our code is by no means optimized, it appears quite competitive with other real-space methods. The CPU time for one time step or fully self-consistent field calculation requires approximately 100 s for one processor on a Cray C-90. Better performance is expected for this algorithm on a parallel machine architecture. Our current CPU time is no doubt an overestimate for the time required for such a calculation since the spherical boundary condition employed here has not been optimized. Cylindrical boundary conditions could reduce this time significantly.

B. Vibrational modes in Si_4

One difficulty in assessing the structures of small clusters as predicted by theory is the lack of experimental data. However, recent experiments on the vibrational spectra of clusters can provide us with very important information about their physical properties. Recently, Raman experiments have been performed on clusters which have been deposited on inert substrates.[25] Since different structural configurations of a given cluster can possess different vibrational spectra, it is possible to compare the vibrational modes calculated for a particular structure with experiment. If the agreement between experiment and theory is good, this is a necessary condition for the theoretically predicted structure.

There are two common approaches for determining the vibrational spectra of clusters. One approach is to calculate the dynamical matrix for the ground-state structure of the cluster:

$$M_{i\alpha,j\beta}=-\frac{1}{m}\frac{\partial^2 E}{\partial R_i^\alpha \partial R_j^\alpha}=\frac{1}{m}\frac{\partial F_i^\alpha}{\partial R_j^\alpha}, \tag{12}$$

where m is the mass of the Si atom, E is the total energy of the system, F_i^α is the force on atom i in the direction α, R_i^α is the α component of coordinate for atom i. We can calculate the dynamical matrix elements by calculating the first-order derivative of force versus atom displacement numerically. By solving for the eigenvalues and eigenmodes of the dynamical matrix, one can obtain the vibrational frequencies and modes for the cluster of interest.[6]

The ground-state structures for small silicon clusters have been determined in previous work via simulated annealing calculations.[15] This approach is quite satisfactory for small silicon clusters, but for larger clusters other approaches such as genetic algorithms might prove to be more useful.[26]

The other approach to determine the vibrational modes is to follow the procedure used for the CO_2 molecule. Namely, one can consider an arbitrary displacement of the cluster and perform a molecular-dynamics simulation using the calculated power spectrum of the kinetic (or binding) energy of the cluster as a function of the MD simulation time. This latter approach has an advantage for large clusters in that one never has to do a mode analysis explicitly. It has the disad-

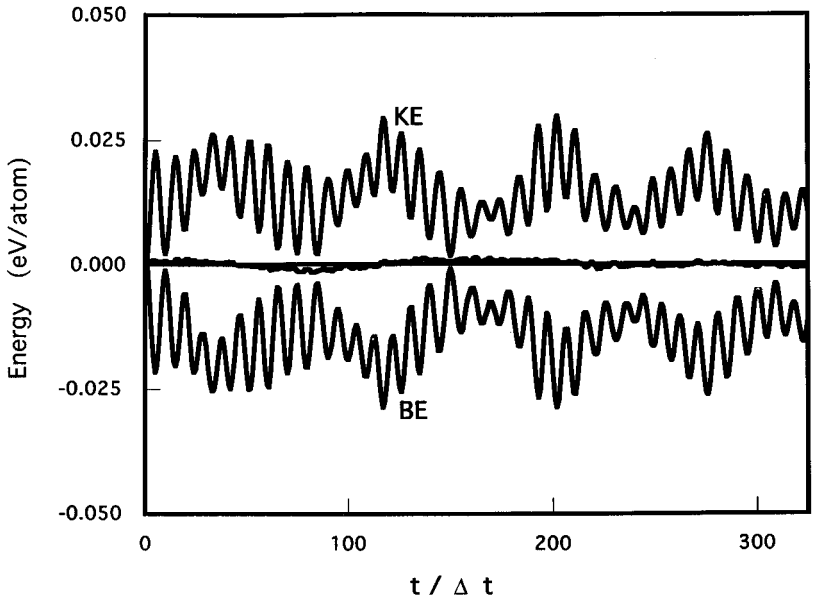

FIG. 4. MD simulation for a Si_4 cluster. The kinetic energy (KE) and binding energy (BE) are shown as a function of the simulation time. The total energy (KE+BE) is also shown with the zero taken as the time average of the total energy. The time step Δt is 3.7 fs.

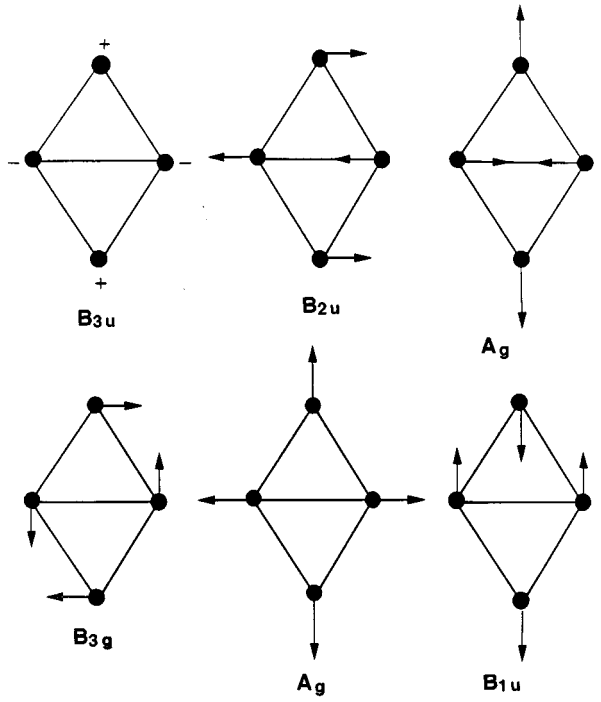

FIG. 5. Normal modes for a Si_4 cluster.

vantage in that the simulation must be performed over a long time to extract all the modes. It may also be difficult to establish appropriate initial displacements so that anharmonic modes are not excited at the expense of the fundamental modes.

The starting geometry was to consider a planar structure for Si_4 as established elsewhere.[15] The grid spacing was taken to be $h=0.7$ a.u. Again, spherical boundary conditions were used with $R_{\max}=10.1$ a.u. We have initiated the simulation by considering a Langevin simulation[27] with a fixed temperature at 300 K. After a few dozen time steps, the Langevin simulation is turned off, and the simulation proceeds following Newtonian dynamics with ''quantum'' forces. This procedure allows a stochastic element to be introduced and establish initial conditions for the simulation without bias toward a particular mode. The time step in the MD simulation was taken to be 3.7 fs or approximately 150 a.u. The simulation was allowed to proceed for 325 time steps. The variation of kinetic and binding energies is given in Fig. 4 as a function of the simulation time. Although some fluctuations of the total energy occurs, these fluctuations are relatively small, i.e., ~ 1 meV, and there is no noticeable drift of the total energy. By taking the power spectrum of either the KE or BE over this simulation time, the vibrational modes can be determined. Even for a relatively simple cluster such as Si_4, the analysis of the modes is nontrival.

In Fig. 5, the fundamental vibrational modes are illustrated. These modes can be identifed with the observed peaks in the power spectrum as illustrated in Fig. 6. The agreement is fairly good; however, one noticeable difference occurs for the (A_g, B_{1u}) mode. Namely, these modes are not resolvable over the simulation time given. This is not an unusual circumstance if the MD simulation times are too short, and if the initial displacements are too large so that the vibrations exceed the harmonic regime. In order to remedy this situation, a ''long'' simulation with small initial displacements was performed to resolve the (A_g, B_{1u}). The kinetic energy fluctuations were adjusted to be less than 0.5 meV and the simulation was performed over a 2 ps simulation time. The spectra for this simulation is illustrated in Fig. 7. Overall the spectra are very similar, but the (A_g, B_{1u}) modes are now resolved. In particular, one notes the splitting between the (A_g, B_{1u}) modes is less than 10 cm^{-1} or about 1 meV.

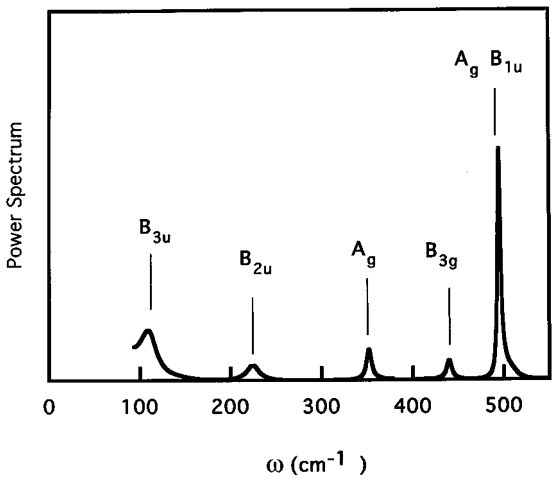

FIG. 6. Power spectrum of the vibrational modes of the Si_4 cluster. The simulation time was 1.2 ps. The intensity of the B_{3g} and (A_g, B_{1u}) peaks has been scaled by 10^{-2}.

A comparison of the calculated vibrational modes from the MD simulation and from a dynamical matrix calculation are listed in Table II. Overall the agreement between the two simulations and the dynamical matrix analysis is quite satisfactory. As expected the simulation which runs longer is in better agreement with the results from the dynamical matrix. In particular, the soft modes such as the B_{3u} mode are sig-

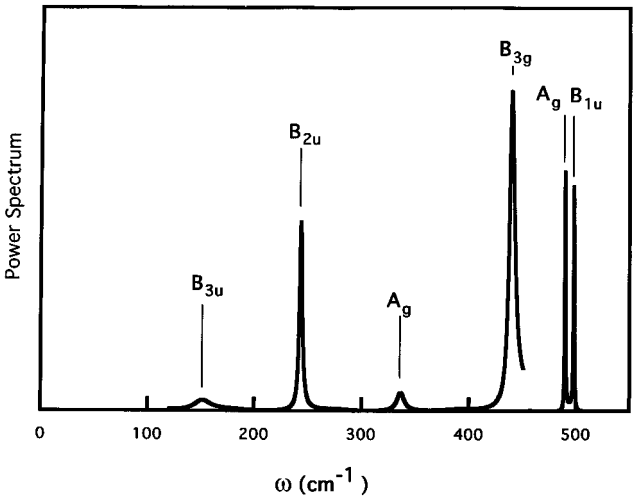

FIG. 7. Power spectrum of the vibrational modes of the Si_4 cluster for a longer simulation (see Fig. 6). The simulation time was 2 ps. The intensity of the (A_g, B_{1u}) peaks has been scaled by 10^{-3}.

TABLE II. Calculated and experimental vibrational frequencies in a Si_4 cluster. See Fig. 5 for an illustration of the normal modes. Three calulations are presented using a real-space grid. The two simulations correspond to (a) ''short'' and (b) ''long'' simulations, see the text and Figs. 6 and 7. The frequencies are given in cm^{-1}.

	B_{3u}	B_{2u}	A_g	B_{3g}	A_g	B_{1u}
Experiment (Ref. 25)			345		470	
Dynamical Matrix	160	280	340	460	480	500
MD simulation (a)	110	225	350	440	495	495
MD simulation (b)	150	250	340	440	490	500
HF (Ref. 29)	117	305	357	465	489	529
LCAO (Ref. 28)	55	248	348	436	464	495

nificantly better for a longer simulation run. The calculated values are also compared to experiment. The calculated frequencies for the two A_g modes are surprisingly close to Raman experiments on silicon clusters.[25] The other allowed Raman line of mode B_{3g} is expected to have a lower intensity and has not been observed experimentally.

The calculated modes (except the lowest mode) are in good accord with other theoretical calculations: a linear combination with atomic orbitals (LCAO) calculation[28] and a Hartree-Fock (HF) calculation.[29] The calculated frequency of the lowest mode, i.e., the B_{3u} mode, is problematic. The general agreement of the B_{3u} mode as calculated by the simulation and from the dynamical matrix is reassuring. Moreover, the real-space calculations agree with the HF value to within $\sim$ 20–30 cm^{-1}. On the other hand, the LCAO method yields a value which is $50-70\%$ smaller than either the real-space or HF calculations. The origin of this difference is not apparent. For a poorly converged basis, vibrational frequencies are often overestimated as opposed to the LCAO result which underestimates the value, at least when compared to other theoretical techniques. Setting aside the issue of the B_{3u} mode, the agreement between the measured Raman modes and theory for Si_4 suggests that Raman spectroscopy can provide a key test for the structures predicted by theory.

V. CONCLUSIONS

We have illustrated in this paper a real-space method which can be used to compute the vibrational modes of molecules and atomic clusters. In particular, we illustrated calculations for the vibrational modes of the CO_2 molecule and a small cluster of silicon (Si_4). Unlike other real-space methods using adaptive grids, this procedure does not require any Pulay corrections for the forces, nor does it suffer from the complication of redefining a grid after each time step of the molecular-dynamics simulation. Our method is based on combining higher-order finite difference methods with *ab initio* pseudopotentials. We also introduced an iterative diagonalization scheme based on preconditioned Krylov techniques. Compared to *plane-wave–supercell methods*, our real-space method is more efficient and simpler to implement.

ACKNOWLEDGMENTS

We would like to acknowledge the support for this work by the National Science Foundation, and by the Minnesota Supercomputer Institute. One of us (J.R.C.) acknowledges very helpful discussions with F. Gygi.

[1] *Quantum Theory of Real Materials*, edited by J.R. Chelikowsky and S.G. Louie (Kluwer, Dordrecht, 1996).

[2] R. Car and M. Parrinello, Phys. Rev. Lett. **55**, 2471 (1985); **60**, 204 (1988); R.M. Wentzcovitch and J.L. Martins, Solid State Commun. **78**, 831 (1991); D.M. Bylander and L. Kleinman, Phys. Rev. B **45**, 9663 (1992); T.A. Arias, M.C. Payne, and J.D. Joannopoulos, *ibid.* **45**, 1538 (1992); N. Binggeli, J.L. Martins, and J.R. Chelikowsky, Phys. Rev. Lett. **68**, 2956 (1992); J.R. Chelikowsky, N. Troullier, and N. Binggeli, Phys. Rev. **49**, 114 (1994).

[3] J.R. Chelikowsky and M.L. Cohen, in *Handbook on Semiconductors*, edited by P.T. Landsberg (Elsevier, Amsterdam, 1992), Vol. 1, Chap. 3, p. 59.

[4] E.L. Briggs, D.J. Sullivan, and J. Bernholc, Phys. Rev. B **52**, R5471 (1995); F. Gygi, *ibid.* **48**, 11 692 (1993); **51**, 11 190 (1995); F. Gygi and G. Galli, *ibid.* **52**, R2229 (1995); S. Wei and M.Y. Chou, Phys. Rev. Lett. (to be published); D.R. Hamann, Phys. Rev. B **51**, 7337 (1995); K. Cho, T.A. Arias, J.D. Joannopoulos, and P.K. Lam, Phys. Rev. Lett. **71**, 1808 (1994); T. Hoshi, M. Arai, and T. Fujiwara, Phys. Rev. B **52**, R5459 (1995); G. Zumbach, N.A. Modine, and E. Kaxiras (unpublished); A.P. Seitsonen, M.J. Puska, and R.M. Nieminen, Phys. Rev. **51**, 14 057 (1995).

[5] F. Gygi and G. Galli, Phys. Rev. B **52**, R2229 (1995).

[6] X. Jing, N. Troullier, J.R. Chelikowsky, K. Wu, and Y. Saad, Solid State Commun. **96**, 231 (1995).

[7] P. Pulay, Mol. Phys. **17**, 197 (1969).

[8] F. Gygi, Phys. Rev. B **51**, 11 190 (1995).

[9] F. Gygi, Phys. Rev. B **48**, 11 692 (1993).

[10] R.P. Feynman, Phys. Rev. **56**, 340 (1939).

[11] J.R. Chelikowsky, N. Troullier, K. Wu, and Y. Saad, Phys. Rev. B **50**, 11 355 (1994).

[12] L. Kleinman and D.M. Bylander, Phys. Rev. Lett. **48**, 1425 (1982).

[13] N. Troullier and J.L. Martins, Phys. Rev. B **43**, 1993 (1991).

[14] C.T. Chan, K.P. Bohnen, and K.M. Ho, Phys. Rev. B **47**, 4771 (1993).
[15] X. Jing, N. Troullier, D. Dean, J.R. Chelikowsky, N. Binggeli, K. Wu, and Y. Saad, Phys. Rev. B **50**, 12 234 (1994).
[16] B. Fornberg and D. Sloan, in *Acta Numerica 1994*, edited by A. Iserles (Cambridge University Press, Cambridge, 1994), pp. 203–267.
[17] D.G. Anderson, J. Assoc. Comp. Mach. **12**, 547 (1965).
[18] B.N. Parlett and Y. Saad, Lin. Alg. Appl. **88/89**, 575 (1987).
[19] Y. Saad, *Numerical Methods for Large Eigenvalue Problems* (Halstead, New York, 1992).
[20] J.M. Ortega, *Introduction to Parallel and Vector Solutions of Linear Systems* (Manchester University Press, Manchester, England, 1992).
[21] G. Bachelet, D.R. Hamann, M. Schlüter, Phys. Rev. B **26**, 4199 (1982).
[22] F. Gygi (private communication).
[23] J.R. Thomas, B.J. DeLeeuw, A. Vacek, T.D. Crawford, Y. Yamaguchi, and H.F. Schaefer III, J. Chem. Phys. **99**, 403 (1993).
[24] L. Pauling, *Nature of the Chemical Bond*, 3rd ed. (Cornell University Press, Ithaca, 1960).
[25] E.C. Honea, A. Ogura, C.A. Murray, Krishnan Raghavacharl, W.O. Sprenger, M.F. Jarrold, and W.L. Brown, Nature (London) **366**, 42 (1993).
[26] D.M. Deaven and K.M. Ho, Phys. Rev. Lett. **75**, 288 (1995).
[27] N. Binggeli, J.L. Martins, and J.R. Chelikowsky, Phys. Rev. Lett. **68**, 2956 (1992).
[28] R. Fournier, S.B. Sinnott, and A.E. DePristo, J. Chem. Phys. **97**, 4149 (1992).
[29] C.M. Rohlfing and K. Raghavachari, J. Chem. Phys. **96**, 2114 (1992).